

# Chaos-based Wireless Communication Resisting Multipath Effect

Jun-Liang Yao, Chen Li, and Hai-Peng Ren

*Shaanxi Key Laboratory of Complex System Control and Intelligent Information Processing,  
Xi'an University of Technology, Xi'an 710048, China*

In additive white gaussian noise (AWGN) channel, chaos has been proved to be optimal coherent communication waveform in the sense of maximizing the signal-to-noise ratio (SNR). Recently, Lyapunov exponent spectrum of the chaotic signals after being transmitted through a wireless channel has also been proved to be unaltered, which paves the way for wireless communication using chaos. In wireless communication system, intersymbol interference (ISI) caused by multipath propagation is one of main obstacles to achieve high bit transmission rate and low bit error rate (BER). How to resist multipath effect is a fundamental problem in chaos-based wireless communication system (CWCS). In this paper, a CWCS is built by transmitting chaotic signals generated by a hybrid dynamical system and filtering the received signal using the corresponding matched filter to decrease noise effect and to detect binary information. We find that the multipath effect can be effectively resisted by regrouping the return map of received signal and setting the corresponding threshold using available information. We show that the optimal threshold is a function of the channel parameters and the transmitted information symbols. Practically, the channel parameters are time-variant, and the future information symbols are unavailable. In this case, a suboptimal threshold (SOT) is proposed, and the BER using the SOT is derived analytically. Numerical experimental results show that the CWCS achieves a very competitive performance even under inaccurate channel parameters.

In recent years, the rapid development of wireless communication technology [1, 2] has dramatically changed the way of our live. As compared with wired communication, the wireless communication channel is more complicated [3]. The wireless channel constraints include limited bandwidth, multipath propagation, Doppler shift and complicated noise, etc.. Firstly, the ISI caused by multipath propagation will increase BER. Secondly, the Doppler shift produced by mobile terminals and scattered clusters will lead to time-variant channel properties. Wireless communication systems have to deal with these problems effectively.

Chaos has attracted lots of attention in the communication field [4–8] since 1990, due to its intrinsic properties suitable for communication applications [9], such as broadband, orthogonality, easy to generate and pseudo-randomness, etc. The maximum rate of communication with chaos was reported in [10, 11]. The channel capacity of chaos-based digital communication in noisy environment was given in [12] and the method for filtering noise in chaotic signal was devised in [13]. Chaotic signals were also used as modulation signals for coherent and non-coherent communications [14]. Since chaos was reported to be successfully used in optic fiber communication system in order to get higher bit transmission rate [15], the researches on communication with chaos has turned to deal with practical communication channels. The wireless channel is such kind of channel with complicated constraints. Among the channel constraints, the limited bandwidth had been considered in chaotic communication system [16], which showed that the BER increased significantly if the bandwidth of the communication channel is low. Some information recovery methods were proposed to decrease the BER in this case [17].

Considering the noise, the recent work in [18–20] proved that chaotic signal was optimal waveform for coherent communication to maximum the SNR. The wireless communication channel constraints make the chaotic signal transmitting through it change dramatically [21]. For using chaos into wireless communication system, a fundamental problem is if the information in chaotic signal is lost after transmitting through the wireless channel. Reference [22] gave an answer to this problem, and showed that the information is not lost.

So far, there is few work to deal with ISI and time-variant channel parameters, caused by multipath propagation and Doppler shift in the CWCS. In the conventional wireless communication system, the known channel state information (CSI) allow the receiver to relief ISI using channel equalization techniques. However, the equalization algorithms are complicated and their performance are susceptible to noise.

In this paper, we find that the multi-branches return map caused by multipath propagation in the CWCS can be regrouped according to the past symbols and multipath effect can be resisted by setting a proper detection threshold for the different groups. The optimal threshold is derived if all symbols and CSI are known in advance, and a SOT is obtained if the future symbols are unknown. Finally, the closed-form expressions for BER of CWCS using the optimal threshold and the SOT are derived. The numerical simulation results demonstrate that the proposed CWCS is robust to the inaccurate CSI. This work proves that CWCS can not only obtain the maximum SNR but also relief the multipath effect, and thus, CWCS might be a competitive alternation of the conventional wireless communication system.

A point-to-point CWCS as shown in Fig. 1 is consid-

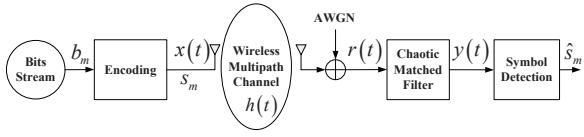


FIG. 1. Schematics of the chaos-based wireless communication system.

ered in this paper. At the transmitter side, the binary bit sequences  $b_m \in [0, 1]$  is encoded to analog signal  $x(t)$  using a hybrid system given by Eq. (1) [23] and the encoding method in [24]

$$\ddot{x} - 2\beta\dot{x} + (\omega^2 + \beta^2)(x - s) = 0, \quad (1)$$

with parameters  $\omega = 2\pi f$  and  $0 < \beta \leq \ln 2$ , where  $f$  is the carrier frequency. The variable  $s = \text{sgn}(x)$  only switches its value when  $\dot{x} = 0$ , keeping its value at other times. The exact analytic solution of Eq. (1) is  $x(t) = \sum_{m=-\infty}^{\infty} s_m p(t - m/f)$ , where  $s_m \in [-1, 1]$  is the bi-polar symbol representing information bit  $b_m$ , the basis function is given by

$$p(t) = \begin{cases} (1 - e^{-\beta})e^{\beta t}(\cos\omega t - \frac{\beta}{\omega}\sin\omega t), & t < 0 \\ 1 - e^{\beta(t-1)}(\cos\omega t - \frac{\beta}{\omega}\sin\omega t), & 0 \leq t < 1/f \\ 0, & t \geq 1/f. \end{cases} \quad (2)$$

The signal  $x(t)$  is transmitted through wireless channel given by  $h(t) = \sum_{l=0}^{L-1} \alpha_l \delta(t - \tau_l)$ , where  $\alpha_l$  and  $\tau_l$  are the attenuation and propagation time delay corresponding to path  $l$  from the transmitter to the receiver,  $\delta(\cdot)$  is the Dirac delta function. The received signal is  $r(t) = h(t) * x(t) + w(t) = \sum_{l=0}^{L-1} \alpha_l x(t - \tau_l) + w(t) = \sum_{l=0}^{L-1} \alpha_l \sum_{m=-\infty}^{\infty} s_m p(t - \tau_l - m/f) + w(t)$ , where  $*$  denotes convolution and  $w(t)$  is AWGN. Assume that the delays  $\tau_l (l = 0, 1, \dots, L-1)$  satisfy  $0 \leq \tau_0 < \tau_1 < \dots < \tau_{L-1}$  and the attenuation  $\alpha_l$  is modeled as an exponential decay  $\alpha_l = e^{-\gamma\tau_l}$  with damping coefficient  $\gamma$  [25].

By sampling  $x(t)$  using frequency  $f$ , and recording as  $x_n = x(n/f)$ , the return map of  $x(t)$  can be given by  $x_{n+1} = e^{\beta}x_n - (e^{\beta} - 1)s_n$ . For a single path channel, the return map of  $r(t)$  is the same as that of  $x(t)$  as shown in Fig. 2(a), where there are two branches plotted using black solid line and black dashed line, respectively. Here, the return map points on the branch plotted with black solid line are corresponding to  $s_n = -1$ , and the points on the black dashed line are corresponding to  $s_n = 1$ . At the  $n$ -th sampled time, the information symbols  $s_n$  can be detected by comparing  $r_n$  with a judgment threshold  $\theta_n$ , then ' $s_n = -1$ ' if ' $r_n \leq \theta_n$ ' and ' $s_n = 1$ ' if ' $r_n > \theta_n$ '. In fact, we can find a *judgment line* (JL), as shown in Fig. 2(a), to distinguish two branches of return map. We define the horizontal distance between the two branches as the *judgment distance* (JD), which

is shown by the distance between two black arrows in Fig. 2(a). In the single path channel,  $\text{JD} = 2(1 - e^{-\beta})$ . The BER under AWGN is depended on both the JD and JL. In Fig. 2(a), the black dotted line  $r_{n+1} = e^{\beta}r_n$  is the optimal JL for distinguishing '1' and '-1', and the corresponding threshold is  $\theta_n = e^{-\beta}r_{n+1}$ .

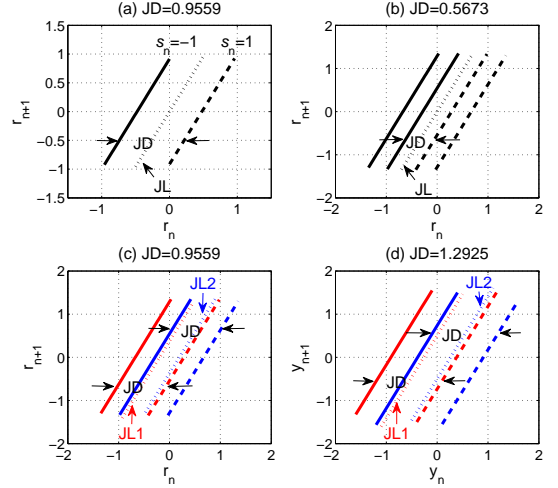


FIG. 2.  $\beta = 0.65$ , return maps for different cases: (a) return map of  $r(t)$  over the single path channel, (b) return map of  $r(t)$  over two paths channel with  $\tau_0 = 0, \tau_1 = 1, \gamma = 0.9$ , (c) regroup of return map in Fig. 2(b), (d) return map of filtered output,  $y(t)$ , over two paths channel.

The return map of  $r(t)$  over two paths channel with propagation delay  $\tau_0 = 0$  and  $\tau_1 = 1$  is given in Fig. 2(b), where more branches appear due to multipath propagation. In fact, the branch number is equal to  $2^L$ , where  $L$  is the multipath number. The further analysis shows that the return map in Fig. 2(b) can be given by  $r_{n+1} = e^{\beta}r_n - (e^{\beta} - 1)(s_n + e^{-\gamma}s_{n-1})$ . The black solid lines and the black dashed lines represent '-1' and '1' as that in Fig. 2(a), in this case  $\text{JD} = 2(1 - e^{-\beta})(1 - e^{-\gamma})$ . More error detection will happen because JD is decreased. The finding in this paper is that these branches caused by multipath propagation can be regrouped into different pairs once the past symbols  $s_{n-i} (i = 1, 2, \dots, L-1)$  are determined. For example, for  $L = 2$ , the branches in Fig. 2(b) can be regrouped as shown in Fig. 2(c), where one past symbol  $s_{n-1}$  is needed to regroup the branches. If  $s_{n-1} = -1$ , the branches pair is corresponding to the red lines, else (i.e.,  $s_{n-1} = 1$ ) the branches pair corresponds to the blue lines, while the solid lines represent ' $s_n = -1$ ' and the dashed lines represent ' $s_n = 1$ ' as well. Note that the branches in Fig. 2(c) are the same as that in Fig. 2(b), but after regrouping the branches that confuse us, we can use separated JLs, so that JD becomes  $2(1 - e^{-\beta})$ , the same as that for the single path channel. In order to have the lowest BER, we use the optimal JLs,  $r_{n+1} = e^{\beta}r_n + (e^{\beta} - 1)e^{-\gamma}s_{n-1}$ , plotted using the dotted lines with different colors in Fig. 2(c), where

the red dotted line corresponds to  $s_{n-1} = -1$  and the blue dotted line corresponds to  $s_{n-1} = 1$ . The thresholds  $\theta_n = e^{-\beta}r_{n+1} + (1 - e^{-\beta})e^{-\gamma}s_{n-1}$ . For more paths, we just need more past symbols to regroup and derive the optimal JLs and the corresponding thresholds.

In the CWCS considered in Fig. 1, the matched filter is used to maximize the SNR. The filtered signal  $y(t)$  is used to detect the information. In the following, we analyze the return map of  $y(t)$  and corresponding thresholds.

The impulse response of matched filter [18] is  $g(t) = p(-t)$  for chaotic signal generated by Eq. (1), the filter output is  $y(t) = g(t) * r(t) = \int_{\tau=-\infty}^{\infty} p(-\tau)r(t - \tau)d\tau = \sum_{l=0}^{L-1} \alpha_l \sum_{m=-\infty}^{\infty} s_m \left( \int_{\tau=-\infty}^{\infty} p(\tau)p(\tau - t + \tau_l + \frac{m-n}{f})d\tau \right) + \int_{\tau=-\infty}^{\infty} p(\tau - t)w(\tau)d\tau$ . Sampling  $y(t)$  at  $t = n/f$  we have

$$\begin{aligned} y_n &= \sum_{l=0}^{L-1} \alpha_l \sum_{m=-\infty}^{\infty} s_m \left( \int_{\tau=-\infty}^{\infty} p(\tau)p(\tau + \tau_l + \frac{m-n}{f})d\tau \right) \\ &+ \int_{\tau=-\infty}^{\infty} p(\tau)w(\tau)d\tau = \sum_{l=0}^{L-1} \sum_{m=-\infty}^{\infty} s_m C_{l,m-n} + W \\ &= \sum_{l=0}^{L-1} s_n C_{l,0} + \sum_{l=0}^{L-1} \sum_{\substack{m=-\infty \\ m \neq n}}^{\infty} s_m C_{l,m-n} + W \\ &= s_n P + I + W. \end{aligned} \quad (3)$$

In Eq. (3), the first term is the expected signal in path  $l$ . The second term  $I$  is filtered ISI from other symbols.  $C_{l,i} = \alpha_l \int_{\tau=-\infty}^{\infty} p(\tau)p(\tau + \tau_l + \frac{i}{f})d\tau$  can be calculated by

$$C_{l,i} = \begin{cases} \alpha_l D(2 - e^{-\beta} - e^{\beta})(A \cos(\omega\tau_l) + B \sin(\omega\tau_l)) & (\tau_l + i/f \geq 1/f) \\ \alpha_l \begin{cases} A(D(2 - e^{-\beta}) - D^{-1}e^{-\beta}) \cos(\omega\tau_l) + \\ B(D(2 - e^{-\beta}) + D^{-1}e^{-\beta}) \sin(\omega\tau_l) \\ + 1 - \tau_l \end{cases} & (0 \leq \tau_l + i/f < 1/f) \\ 0 & (\text{others}), \end{cases} \quad (4)$$

where  $A = \frac{\omega^2 - 3\beta^2}{4\beta(\omega^2 + \beta^2)}$ ,  $B = \frac{3\omega^2 - \beta^2}{4\omega(\omega^2 + \beta^2)}$  and  $D = e^{-\beta(\tau_l + \frac{i}{f})}$ .

Since  $C_{l,i}$  is a geometric sequence (for increasing  $i$ ) with common ratio equal to  $e^{-\beta}$ , when  $\tau_l + i/f \geq 1/f$ , the return map of  $y(t)$  can be denoted as  $y_{n+1} = e^{\beta}y_n - (e^{\beta} - 1) \sum_{l=0}^{L-1} s_{n+[\lceil -\tau_l f \rceil]} C_{l, [\lceil -\tau_l f \rceil]}$ , where  $\lceil -\tau_l f \rceil$  represents the ceiling of  $-\tau_l f$ . For the two path channel case in Fig. 2(c), the return map of  $y(t)$  is given in Fig. 2(d). The solid lines represent  $s_n = -1$  and the dashed lines represent  $s_n = 1$ . As we do for the return map of  $r(t)$ , the multiple branches of the return map of  $y(t)$  in Fig. 2(d) can be also regrouped, where the red lines correspond to  $s_{n-1} = -1$  and the blue lines correspond to  $s_{n-1} = 1$ . The optimal JLs,  $y_{n+1} = e^{\beta}y_n - (e^{\beta} - 1)s_{n-1}C_{1,-1}$ , for different groups

are plotted using the dotted line with corresponding colors. In this case,  $JD = 2(1 - e^{-\beta})C_{0,0}$ . For  $L$  paths channel, the optimal JLs are  $y_{n+1} = e^{\beta}y_n - (e^{\beta} - 1) \sum_{l=1}^{L-1} s_{n+[\lceil -\tau_l f \rceil]} C_{l, [\lceil -\tau_l f \rceil]}$ , and the optimal threshold are  $\theta_n = e^{-\beta}y_{n+1} + (1 - e^{-\beta}) \sum_{l=1}^{L-1} s_{n+[\lceil -\tau_l f \rceil]} C_{l, [\lceil -\tau_l f \rceil]}$ . From the return map of  $y(t)$  and Eq. (3),  $\theta_n$  can be given by

$$\theta_n = I = \sum_{l=0}^{L-1} \sum_{\substack{m=-\infty \\ m \neq n}}^{\infty} s_m C_{l,m-n}. \quad (5)$$

The right-hand side in Eq. (5) is the ISI, which contains both the past symbols  $s_m (m < n)$  and the future symbols  $s_m (m > n)$ . According to Eq. (4), only  $C_{l,m-n}$  with index  $m \geq n + \lceil -\tau_l f \rceil$  will be non-zero. Then the ISI from past symbols can be denoted as  $I_{past} = \sum_{l=0}^{L-1} \sum_{m=n+[\lceil -\tau_l f \rceil]}^{n-1} s_m C_{l,m-n}$ . If we know the CSI,  $C_{l,m-n}$  can be calculated using Eq. (4). Before detecting  $s_n$ , the past symbols  $s_m (m = n + \lceil -\tau_l f \rceil, \dots, n-1)$  have been decoded, thus  $I_{past}$  can be calculated. The ISI from future symbols is  $I_{future} = K \sum_{m=n+1}^{\infty} s_m e^{-\beta(m-n)/f}$ , where  $K = \sum_{l=0}^{L-1} \alpha_l (2 - e^{-\beta} - e^{\beta}) e^{-\beta\tau_l} (A \cos(\omega\tau_l) + B \sin(\omega\tau_l))$  depends on the CSI. With the assumption that  $p(s_m = 1) = p(s_m = -1) = 1/2$ ,  $I_{future}$  is uniform distribution in the range given by  $[-|\frac{K}{e^{\beta/f}-1}|, |\frac{K}{e^{\beta/f}-1}|]$ . Because  $I_{future}$  cannot be calculated at the current time, so  $I_{past}$  is a SOT based on available information.

The third term in Eq. (3),  $W = \int_{\tau=-\infty}^{\infty} p(\tau)w(\tau)d\tau$ , is the filtered noise. If  $w(\tau)$  is AWGN with zero mean, then  $W$  is also AWGN with zero mean [26]. Assuming the variance of  $W$  is  $\sigma_W^2$ , then  $y_n$  is a Gaussian random variable with conditional probability distribution

$$p(y_n | s_n, I) = \frac{1}{\sqrt{2\pi\sigma_W^2}} e^{-\frac{|y_n - s_n P - I|^2}{2\sigma_W^2}}. \quad (6)$$

From Eq. (6), the BER using the optimal threshold  $\theta_n = I$  for detecting  $s_n$  from  $y_n$  is

$$p(\text{error} | \theta_n = I) = \frac{1}{2} \text{erfc} \left( \frac{P}{\sqrt{2\sigma_W^2}} \right), \quad (7)$$

in which  $\text{erfc}(\cdot)$  is the complementary error function,  $P^2/(2\sigma_W^2)$  is the filtered SNR. The BER using SOT, i.e.,  $\theta_n = I_{past}$ , for detecting  $s_n$  from  $y_n$  is given as

$$\begin{aligned} p(\text{error} | \theta_n = I_{past}) &= \frac{e^{\beta/f} - 1}{4|K|} \int_{-\frac{|K|}{e^{\beta/f}-1}}^{\frac{|K|}{e^{\beta/f}-1}} \text{erfc} \left( \frac{P + I_{future}}{\sqrt{2\sigma_W^2}} \right) dI_{future} \\ &= \sqrt{2\sigma_W^2} \frac{e^{\beta/f} - 1}{4|K|} \left( x \cdot \text{erfc}(x) - \frac{e^{-x^2}}{\sqrt{\pi}} \right) \Bigg|_{\frac{P - \frac{|K|}{e^{\beta/f}-1}}{\sqrt{2\sigma_W^2}}}^{\frac{P + \frac{|K|}{e^{\beta/f}-1}}{\sqrt{2\sigma_W^2}}}. \end{aligned} \quad (8)$$

Equation (7) and (8) are the analytical BER using the optimal threshold and the SOT, respectively.

In the conventional wireless communication system, the complicated equalization is required to decrease the multipath effect. When both the performance and algorithm complexity are considered, minimum mean square error (MMSE) equalizer is an excellent choice [27]. To analyze the performance of the proposed CWCS, the simulation is performed using different thresholds, including  $\theta = 0$  (without consideration of multipath effect),  $\theta = 0$  combined with MMSE,  $\theta = I_{past}$  and  $\theta = I$ . The BER lower bound of the single path channel [18] is also given for comparison, as shown in Fig. 3.

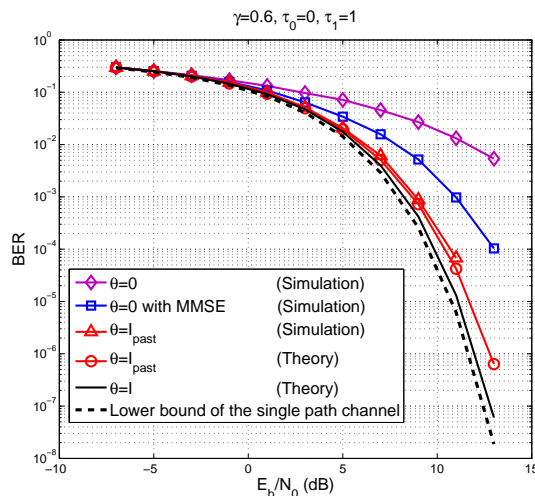


FIG. 3. BER comparison results. Black solid line is the theoretical BER using the optimal threshold  $\theta = I$ , red solid line with circle markers is the theoretical BER using  $\theta = I_{past}$ , red solid line with upper triangular markers is the simulation result using  $\theta = I_{past}$ , blue solid line with square markers is the simulation result using  $\theta = 0$  combined with MMSE, violet solid line with diamond markers is the simulation result using  $\theta = 0$ . Black dashed line is the BER lower bound for the single path channel.

In Fig. 3, we assume energy cost per bit is  $E_b = 1$ , two paths with propagation delay  $\tau_0 = 0$ ,  $\tau_1 = 1$  and damping coefficient  $\gamma = 0.6$ . The simulation results are obtained by averaging over 50000 trials. As shown in Fig. 3, when  $\theta = 0$ , the CWCS has the worst BER, because the multipath effect is completely ignored under such condition. BER is reduced by introducing MMSE equalization. But it is obvious that BER of SOT,  $\theta = I_{past}$ , is not only lower than the above two methods evidently, but also close to the optimal threshold  $\theta = I$  and the lower bound of single path channel with respect to different  $E_b/N_0$ . Therefore, the CWCS using the SOT decreases the multipath effect efficiently.

In the CWCS, the accurate CSI are required for equalization or calculating threshold  $\theta$ . In the following part, we analyze the effect of the inaccurate CSI due to the

TABLE I. Required  $E_b/N_0$  (dB) for BER =  $10^{-3}$

Required $E_b/N_0$ (dB)	$\varepsilon = 0.3$	$\varepsilon = 0.2$	$\varepsilon = 0.1$	$\varepsilon = 0$
$\theta = I$ (theory)	8	8	8	8
$\theta = I_{past}$ (theory)	8.5	8.5	8.5	8.5
$\theta = I_{past}$ (simu.)	9.7	9.2	8.9	8.7
$\theta = 0$ with MMSE (simu.)	12	11.5	11.3	11
$\theta = 0$ (simu.)	16	16	16	16

imperfect channel estimation or time-variant channel including Doppler effects. We assume that the estimated channel  $\hat{h} = h + \Delta h$  is different from the accurate channel  $h$ , where  $\Delta h$  is the channel estimation error uniformly distributed in the range  $[-\varepsilon h, \varepsilon h]$ . Table 1 gives the required  $E_b/N_0$  for BER =  $10^{-3}$  under different  $\varepsilon$ . In Table 1, five methods in Fig. 3 are given for comparison. Both the theoretical BER using  $\theta = I$  and  $\theta = I_{past}$  are not affected by the inaccurate CSI. The simulation BER using  $\theta = 0$  is also unchanged with the variant channel error, because the estimated CSI is not involved at all in this result. For  $\theta = I_{past}$  and  $\theta = 0$  with MMSE, the simulation results are affected by the channel error, the higher  $\varepsilon$ , the higher required  $E_b/N_0$ , due to the inaccurate channel parameter  $\hat{h}$  used. However, the channel estimation error doesn't play a big role on  $E_b/N_0$ , because only 1dB gap between  $\varepsilon = 0.3$  and  $\varepsilon = 0$ . The result shows that the SOT, i.e.,  $\theta = I_{past}$ , is robust to channel error, and can efficiently decrease BER caused by the multipath.

To summarize, the influence of multipath on information decoding using the return map of chaotic signal is firstly reported in this paper. We find that the multi-branches return map of the received signal (and the filtered signal) can be regrouped and the different JLs can be used to decrease the BER caused by the multipath propagation. We obtain the optimal threshold  $\theta = I$  for the filtered signal, whose BER is very close to the lower bound of BER for the single path channel. Considering that the future information symbols are unavailable for detecting the current symbol, we propose a SOT. The analytical expression of BER using SOT is derived, which contains the channel parameters and the past symbols, and thus can be obtained by channel estimation and symbols detected in the past. Simulation and numerical analysis results show that the SOT can eliminate the major part of multipath effect, and it works well even in the time-variant wireless channel. The results in this paper, together with the results in [22], show the merits of CWCS including: 1) a simple encoding method with less energy consumption by using impulse control [23, 24]; 2) noise like signal is transmitted in the wireless channel, which is environment friendly due to no frequency pollution involved; 3) a simple decoding method resists the multipath effect and achieves a very competitive BER performance.

This work is supported by NSFC (61401354, 61172070), Innovative Research Team of Shaanxi

Province (2013KCT-04), Key Basic Research Fund of Shaanxi (2016JQ6015).

- 
- [1] A. Goldsmith, *Wireless Communications* (Cambridge University Press, 2005).
- [2] D. Tse and P. Viswanath, *Fundamentals of wireless communication* (Cambridge University Press, 2005).
- [3] A. F. Molisch and F. Tufvesson, *IEICE Transactions on Communications* **E97.B**, 2022 (2014).
- [4] S. Wang, J. Kuang, J. Li, Y. Luo, H. Lu, and G. Hu, *Phys. Rev. E* **66**, 065202 (2002).
- [5] S. Boccaletti, A. Farini, and F. T. Arecchi, *Phys. Rev. E* **55**, 4979 (1997).
- [6] E. M. Bollt, *International Journal of Bifurcation and Chaos* **13**, 269 (2003).
- [7] H. Leung, H. Yu, and K. Murali, *Phys. Rev. E* **66**, 036203 (2002).
- [8] R. M. Nguimdo, P. Colet, L. Larger, and L. Pesquera, *Phys. Rev. Lett.* **107**, 034103 (2011).
- [9] M. Eisenkraft, R. Attux, and R. Suyama, *Chaotic Signals in Digital Communications* (CRC Press, Boca Raton, FL, 2013).
- [10] M. S. Baptista and L. López, *Phys. Rev. E* **65**, 055201 (2002).
- [11] S. Hayes, C. Grebogi, and E. Ott, *Phys. Rev. Lett.* **70**, 3031 (1993).
- [12] E. M. Bollt, Y.-C. Lai, and C. Grebogi, *Phys. Rev. Lett.* **79**, 3787 (1997).
- [13] E. Rosa, Jr., S. Hayes, and C. Grebogi, *Phys. Rev. Lett.* **78**, 1247 (1997).
- [14] G. Kaddoum, *IEEE Access* **4**, 2621 (2016).
- [15] A. Argyris, D. Syvridis, L. Larger, V. Annovazzi-Lodi, P. Colet, I. Fischer, J. Garcia-Ojalvo, C. R. Mirasso, L. Pesquera, and K. A. Shore, *Nature* **438**, 343 (2005).
- [16] L. Zhu, Y.-C. Lai, F. C. Hoppensteadt, and E. M. Bollt, *Chaos* **13**, 410 (2003).
- [17] H. P. Ren, M. S. Baptista, and C. Grebogi, *International Journal of Bifurcation and Chaos* **22**, 1250199 (2012).
- [18] N. J. Corron, J. N. Blakely, and M. T. Stahl, *Chaos* **20** (2010).
- [19] S. D. Cohen and D. J. Gauthier, *Chaos* **22**, 033148 (2012).
- [20] N. J. Corron and J. N. Blakely, *Proceedings of the Royal Society of London A: Mathematical, Physical and Engineering Sciences* **471** (2015).
- [21] H. P. Ren, M. S. Baptista, and C. Grebogi, “Robustness of chaos to multipath propagation media,” in *Chaotic Signals in Digital Communications*.
- [22] H. P. Ren, M. S. Baptista, and C. Grebogi, *Phys. Rev. Lett.* **110**, 184101 (2013).
- [23] C. Grebogi, M. S. Baptista, and H. P. Ren, “Wireless communication method using a chaotic signal,” United Kingdom Patent Application No.1307830.8 (2015), H. P. Ren, M. S. Baptista, C. Grebogi, “Wireless communication and transmission encoding method”, P. R. China Patent Application No.201410203969.9 (2014).
- [24] H. P. Ren, C. Bai, J. Liu, M. S. Baptista, and C. Grebogi, *Chaos* **26**, 083117 (2016).
- [25] Due to the form of  $p(t)$  in Eq. (2) and time delay  $\tau_i$ , received signal  $r(t)$  depends on not only the current and future symbols, but also the past symbols.
- [26] J. N. Blakely, D. W. Hahs, and N. J. Corron, *Physica D: Nonlinear Phenomena* **263**, 99 (2013).
- [27] M. Tuchler, A. C. Singer, and R. Koetter, *IEEE Transactions on Signal Processing* **50**, 673 (2002).